Translational Stroke Research (2018) 9:608–621
https://doi.org/10.1007/s12975-018-0612-4

ORIGINAL ARTICLE

ICAM-1^{null} C57BL/6 Mice Are Not Protected from Experimental Ischemic Stroke

Gaby U. Enzmann[1] · Sofia Pavlidou[1] · Markus Vaas[2,3] · Jan Klohs[2,3] · Britta Engelhardt[1]

Received: 20 October 2017 / Revised: 19 January 2018 / Accepted: 19 January 2018 / Published online: 4 February 2018

Abstract

Accumulation of neutrophils in the brain is a hallmark of cerebral ischemia and considered central in exacerbating tissue injury. Intercellular adhesion molecule (ICAM)-1 is upregulated on brain endothelial cells after ischemic stroke and considered pivotal in neutrophil recruitment as ICAM-1-deficient mouse lines were found protected from experimental stroke. Translation of therapeutic inhibition of ICAM-1 into the clinic however failed. This prompted us to investigate stroke pathogenesis in Icam1^{tm1Alb} C57BL/6 mutants, a true ICAM-1^{null} mouse line. Performing transient middle cerebral artery occlusion, we found that absence of ICAM-1 did not ameliorate stroke pathology at acute time points after reperfusion. Near-infrared imaging showed comparable accumulation of neutrophils in the ischemic hemispheres of ICAM-1^{null} and wild type C57BL/6 mice. We also isolated equal numbers of neutrophils from the ischemic brains of ICAM-1^{null} and wild type C57BL/6 mice. Immunostaining of the brains showed neutrophils to equally accumulate in the leptomeninges and brain parenchymal vessels of ICAM-1^{null} and wild type C57BL/6 mice. In addition, the lesion size was comparable in ICAM-1^{null} and wild type mice. Our study demonstrates that absence of ICAM-1 neither inhibits cerebral ischemia-induced accumulation of neutrophils in the brain nor provides protection from ischemic stroke.

Keywords Blood-brain barrier · Endothelium · Focal ischemia · Leukocytes · Vascular biology

Introduction

The neurovascular unit (NVU) characterizes the functional connection between the constituents of the vascular compartment and the central nervous system (CNS) [1]. Its anatomical substrate is the blood-brain barrier (BBB), a composition of highly specialized endothelial cells studded with complex tight junctions interconnecting adjacent cells, pericytes, perivascular antigen-presenting cells, extracellular matrix proteins, glial cells, and neurons. The capillary BBB serves as a physical barrier for the CNS permitting uptake of vital substrates but simultaneously restricting the passage of blood-borne components potentially causing CNS dysfunction. At the post-capillary venule level, the BBB limits under steady-state conditions the migration of immune cells to few cells of the adaptive immune system serving the purpose of immunosurveillance [2]. Changes in the NVU, manifested by upregulation of adhesion molecules or increased BBB permeability, are observed in various neurological disorders (reviewed in [3]) and are often accompanied by inflammatory cell recruitment into the brain [4]. Trafficking of leukocytes into the CNS occurs at the level of the post-capillary venules [5] and is mediated by a multistep cascade initiated by tethering and subsequent rolling of leukocytes along the vessel wall, which results in their arrest and crawling on the endothelial surface (reviewed in [4]) allowing to search for sites for their transcellular or paracellular diapedesis [4].

The innate immune system is ascribed a key role in initiation of inflammation during acute cerebral ischemia. Danger-

Electronic supplementary material The online version of this article (https://doi.org/10.1007/s12975-018-0612-4) contains supplementary material, which is available to authorized users.

✉ Britta Engelhardt
bengel@tki.unibe.ch

[1] Theodor Kocher Institute, University of Bern, Freiestrasse 1, 3012 Bern, Switzerland

[2] Institute for Biomedical Engineering, ETH and University of Zurich, 8093 Zurich, Switzerland

[3] Neuroscience Center Zurich, University of Zurich and ETH Zurich, Zurich, Switzerland

associated molecular patterns such as high-mobility group box-1 and heat shock proteins are released from dying neurons, stimulate the inflammasome in inflammatory cells and induce the secretion of pro-inflammatory cytokines (reviewed in [6]). Release of TNF-α and IL-1β by perivascular macrophages, microglia, astrocytes, and endothelial cells (reviewed in [7]) promotes upregulation of adhesion molecules including intercellular adhesion molecule (ICAM)-1 on brain endothelial cells paving the way for leukocyte interaction with the ischemic BBB [8–10]. Neutrophils are the first leukocyte subpopulation accumulating in the ischemic brain [11] and are thought to exacerbate tissue injury by exerting oxidative stress to surviving neurons in the penumbral region [12, 13]. Contrary to this general view, others and we have recently observed in brain tissue from ischemic stroke patients and from mice after experimental cerebral ischemia that neutrophils fail to migrate into the brain parenchyma and rather accumulate in the leptomeninges and within the confines of the NVU without any direct contact to hypoxic neurons [9, 14].

Previous studies have identified endothelial ICAM-1 as a potential therapeutic target for the treatment of ischemic stroke. The observation of cerebral protection upon stroke in ICAM-1-deficient mice was interpreted such that it confers inhibition of LFA-1/ICAM-1-mediated neutrophil recruitment into the CNS [15, 16]. Translation of this therapeutic approach into the clinic has however failed. In the Enlimomab phase III clinical trial, a monoclonal murine anti-human ICAM-1 antibody (R6.5) designed to inhibit ICAM-1-mediated neutrophil adhesion to cerebral microvessels during the acute phase of stroke caused neurological deficits and even increased mortality [17]. In retrospect, sensitization against murine epitopes and in vivo activation of neutrophils by the antibody was held accountable for the adverse effects [18]. On the other hand, the ICAM-1 mutants employed in the pre-clinical stroke studies, which were created by disrupting either exon 4 ($Icam1^{tm1Jcgr}$) [19] or exon 5 ($Icam1^{tm1Bay}$) [20] of the ICAM-1 gene, have been shown to still express functional soluble splice variants of ICAM-1 [21] that influence leukocyte adhesion and migration [22] and thus affected the outcome of autoimmune neuroinflammation [23, 24].

In light of these controversial results regarding the role of ICAM-1 in stroke pathogenesis in general and in neutrophil accumulation in the NVU in particular, we decided to study ischemic stroke using the model of transient middle cerebral artery occlusion (tMCAO) in a truly ICAM-1-deficient mouse strain to avoid potential misinterpretations due to the presence of protein variants produced from the incompletely deleted exons in mice carrying other mutated alleles [19, 20]. The $Icam1^{tm1Alb}$ mutant mouse used in the present study contains a deletion of the entire ICAM-1 coding region precluding production of any splice variants. Therefore, this ICAM-1 mutant mouse represents a true ICAM-1 null allele [25] lacking expression of any alternate splice variants coding for ICAM-1 protein isoforms [26].

Material and Methods

Mice

$ICAM\text{-}1^{null}$ mice ($Icam1^{tm1Alb}$) were generated by deletion of the entire coding region of the ICAM-1 gene [25] and were kindly provided by D. Bullard and S. Barnum (University of Birmingham, Alabama, USA). In contrast to the ICAM-1 mouse mutants carrying insertions of a neomycin resistance gene within the fourth ($Icam1^{tm1Jcgr}$) or fifth exon ($Icam1^{tm1Bay}$) of ICAM-1, these $ICAM\text{-}1^{null}$ C57BL/6 mice do not express any functional soluble splice variants of ICAM-1 and are thus true $ICAM\text{-}1^{null}$ mice [24]. Thymus sections of $ICAM\text{-}1^{null}$ mice were assessed by immunohistology side by side with tissue samples from the $Icam1^{tm1Jcgr}$ mutant mice in our laboratory. Detection of ICAM-1 immunostaining in the thymus of the $Icam1^{tm1Jcgr}$ mutant mouse confirmed the presence of splice variants, while lack of ICAM-1 detection in the $ICAM\text{-}1^{null}$ mouse indicated absence of any alternate spliced isoforms in this mutant corroborating findings by van den Engel et al. [21].

$ICAM\text{-}1^{null}$ mice were backcrossed for 15 generations to the C57BL/6J background with C57BL/6J mice obtained from Janvier Laboratories (Saint Berthevin, France).

A total of 63 male $ICAM\text{-}1^{null}$ C57BL/6 and 52 C57BL/6 wild type littermates were subjected to cerebral ischemia and sham surgery, respectively. The experimental design of our study is outlined in Fig. 1. The age of the animals ranged from 12 to 30 weeks with a weight of 19–27 g. Among them, eight mice of either genotype had to be excluded from further analysis and were sacrificed due to excessive (6) or insufficient (2) lesions.

Transient Middle Cerebral Artery Occlusion

Transient ischemia using the intraluminal filament model [27] was performed on isoflurane-anesthetized male $ICAM\text{-}1^{null}$ C57BL/6 and wild type C57BL/6 littermates. A third mouse group was subjected to sham occlusion. Appropriate analgesia during anesthesia was ensured by a single subcutaneous injection of Buprenorphine (0.1 mg/kg body weight) 60 min prior surgery and maintained for the following 2 days. To account for blood loss, mice received a total of 1 ml 0.9% saline prior surgery. Reperfusion (RP) was permitted for 6, 12, 24, 48, and 72 h post-ischemia. The described lesion paradigm caused an extensive damage to the unilateral basal ganglia and the adjacent neocortex. For clinical scoring, mice were examined for forelimb flexion and body posture maintenance [28]. Mice achieving a score of 1 (failure to extent the ipsilateral and/or

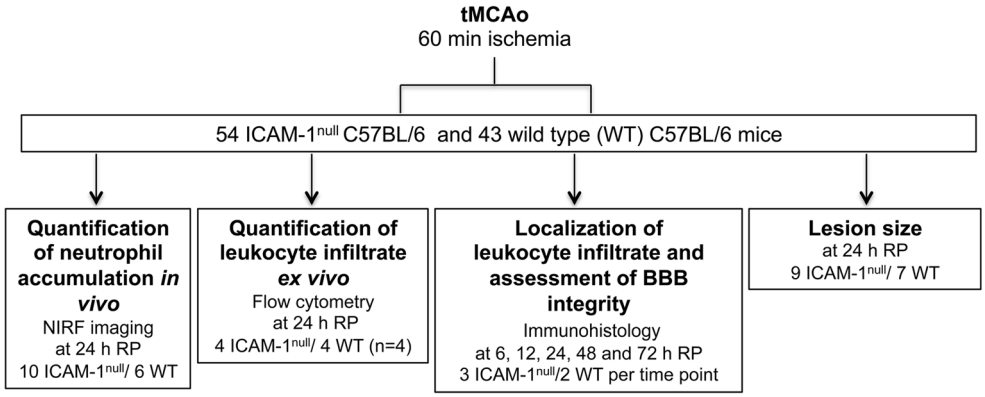

Fig. 1 The flow chart summarizes the experimental setup and the number of mice analyzed at different stages of the study. The latter includes eight animals, which had to be excluded from further analysis. Additional 18 mice underwent sham surgery and are not listed here

contralateral paw) or 2 (circling to the paretic side) were included into further analysis. Mice exhibiting no deficit (score 0) or falling to the paretic side (score 3) were excluded from further analysis.

Adoptive Transfer of Fluorescent-Labeled Neutrophils

Neutrophils were isolated from the bone marrow of C57BL/6 mice and labeled for near-infrared fluorescence (NIRF) imaging as previously described [29, 30]. Isolated neutrophils were incubated in HBSS (0.2×10^6 cells/10 μl) with 25 μg/ml of LIPO-6S-IDCC (Freie Universität Berlin, Germany) at RT for 20 min. A total of 7.5×10^6 LIPO-6S-IDCC-labeled neutrophils in a volume of 100 μl were adoptively transferred by intravenous injection into the tail vein of each non-transgenic littermate and ICAM-1^{null} mouse 15 min prior conducting tMCAO. Altogether, 10 ICAM-1^{null} C57BL/6 and six wild type mice were investigated.

NIRF Imaging for Quantitative Assessment of Neutrophil Accumulation in the Brain

NIRF imaging was performed at 18 h after reperfusion [30]. Mice were anesthetized with 1.5–2% isoflurane in an oxygen/air mixture (1:4). The skin overlying the head was shaved and depilated. NIRF imaging was performed with the Maestro 500 multispectral imaging system (Cambridge Research & Instruments Inc., Woburn, USA). A band-pass filter (615–665 nm) was used for excitation. A CCD camera fitted with a longpass filter (700 nm) was employed to detect the fluorescence signal. Fluorescence emission images were acquired by incrementally increasing the excitation wavelengths over the indicated range.

NIRF images were subjected to spectral unmixing using the CRi Maestro Image software. Regions of interest (ROI) were manually drawn over the right and left hemisphere of the brain excluding none cerebral areas as described earlier [30]. The average fluorescence intensity of all pixels within the ROI was measured and divided by the factor of their area.

Tissue Processing

At various time points of RP, mice were deeply anesthetized with isoflurane and perfused with 1% paraformaldehyde in PBS, pH 7.4. Brains were dissected, embedded in Tissue-Tek (OCT compound), and frozen in a dry ice-cooled 2-methylbutane bath. A total of 15 ICAM-1^{null} and 10 wild type C57BL/6 mice, i.e., three and two mice per genotype and RP time, respectively, were used for staining purposes.

Immunostaining and immunofluorescence (IF) were performed on 6-μm cryostat sections spanning the extent of the lesion. Sections were fixed in – 20 °C acetone, stained using a three-step immunoperoxidase staining kit, and developed with AEC substrate (Vectastain, Vector). Finally, sections were counterstained with Mayer's Hemalaun. For IF, secondary antibodies, e.g., goat anti-rat IgG and anti-rabbit IgG conjugated with Alexa Fluor 488, Cy3, or AMCA (Molecular Probes), were used, respectively. Biotinylated mouse IgG was developed with streptavidin-conjugated DyLight 488 (Jackson ImmunoResearch). Sections were assessed using a Nikon Eclipse E600 microscope equipped with a digital camera.

Antibodies

The following primary antibodies were employed for immunohistochemistry, IF, and flow cytometry analysis: rat anti-mouse ICAM-1 (25ZC7) [31], rat anti-mouse ICAM-2 (3C4) (BD Pharmingen), rat anti-mouse vascular cell adhesion molecule (VCAM-1) (2A11.12) [32], rat anti-mouse PECAM-1 (Mec13.3) (BioLegend), rat anti-mouse PSGL-1 (4RA10) [33], rat anti-mouse CD11b/Mac-1 (M1/70) (BD Pharmingen), rat anti-mouse CD4 (GK1.5) (BD Pharmingen), rat anti-mouse CD8 (Lyt2) (BD Pharmingen), rat anti-mouse CD41 (BD Pharmingen), rat anti-mouse CD45 (M1/9) (BD Pharmingen), rat CD45R/B220 (RA3-6B2) (BD Pharmingen), rat anti-mouse F4/80 (BD Pharmingen), rat anti-mouse 7/4 (AbD Serotec), rat anti-mouse Ly6G (1A8) [34], rat anti-mouse Ter-119 (BD Pharmingen), rabbit anti-mouse P-selectin [35], rabbit pan-laminin (DAKO Cytomation), rabbit

anti-fibrinogen (LSBio), goat anti-mouse CD3ε (Santa Cruz), and biotinylated murine IgG (Vector). Rat anti-human CD44 (huHERMES-1, 9B5) [36], rat, goat, and rabbit IgG were applied as isotype controls.

Lesion Volumetry

Five-micrometer thick sections were made at stereotactic coordinates of Bregma + 2.80, + 1.54, + 0.14, − 1.94, and − 4.60 ± 0.1 mm. Slides were dried overnight and post-fixed in acetone at − 20 °C for 10 min. Next, the sections were stained with hematoxylin-eosin (H&E) using an automated Tissue-Tek® Prisma™ & FIlm™ slide stainer (Sakura, Germany) and digitized with a Pannoramic Digital Slide Scanner (3DHISTEC, Hungary) at ×20. ROI were drawn manually around the infarct area, the non-affected tissue of the ipsilateral hemisphere (NAT), and the contralateral hemisphere (CLH) using NDP.view software (Hamamatsu Photonics K.K., Japan). Cerebral lesion volumes were calculated as follows:

$$V = \mathrm{Vol}(\mathrm{ROI}_{+2.80}) + 2*(\mathrm{Vol}(\mathrm{ROI}_{+1.54}) + \mathrm{Vol}(\mathrm{ROI}_{+0.14}) + \mathrm{Vol}(\mathrm{ROI}_{-1.96})) + \mathrm{Vol}(\mathrm{ROI}_{-4.60})$$

To calculate the infarct volume without edema $V_{(i)}$, the volume of NAT was subtracted from the volume of CLH. Previous calculation of the sample size with a power of 0.9 and an alpha equaling 0.05 for non-normal distributed data required assessment of 8 mice per genotype.

Flow Cytometry

Inflammatory cells from the ischemic ipsilateral and from the contralateral hemisphere were isolated and stained as previously described [32, 37]. In detail, four mice per genotype of four independent experiments were subjected to tMCAO and perfused with PBS, pH 7.4. Ischemic and contralateral cerebra were separated, mechanically dissociated, consecutively digested with collagenase VIII and DNAse I, and filtered. Cells were separated by centrifugation through a Percoll gradient. Leukocytes were collected from the interphase and stained for CD45 and Ly6G to identify neutrophils. Flow cytometry was performed using a FACSCalibur. CellQuest (Becton Dickinson) and FlowJo (Tree Star Inc.) software were employed for data analysis.

Statistical Analysis

Statistical analysis was performed using GraphPad Prism software (GraphPad, San Diego, CA, USA). Data are presented as mean ± SD, and Student's *t* test was performed to compare different data sets.

Results

Absence of ICAM-1 Does Not Affect Neutrophil Accumulation in the Brain Following Cerebral Ischemia and Reperfusion in Live Mice

We first asked if absence of ICAM-1 reduced the accumulation of $CD45^+/Ly6G^+$ neutrophils following tMCAO and reperfusion. We have previously shown that NIRF imaging provides a versatile tool to non-invasively study dynamics of neutrophil accumulation into the mouse brain after experimental cerebral ischemia [30]. Taking thus advantage of NIRF, we first tracked the accumulation of adoptively transferred bone marrow-derived fluorophore labeled $Ly6G^+$ neutrophils in $ICAM1^{null}$ and wild type C57BL/6 mice after tMCAO. To our surprise, we did not detect any differences in the normalized NIRF fluorescence intensities between $ICAM1^{null}$ and wild type C57BL/6 littermates 18 h after reperfusion, ($ICAM1^{null}$ C57BL/6 0.0046 ± 0.0021 versus wild type C57BL/6 0.0032 ± 0.0024, $P > 0.05$) (Fig. 2a–b) indicating that absence of ICAM-1 does not affect neutrophil accumulation in the ischemic brain.

To substantiate this unexpected finding, we next quantified the numbers of neutrophils isolated from the ipsilateral and contralateral brain hemispheres of wild type and $ICAM\text{-}1^{null}$ C57BL/6 mice after 60 min of tMCAO and 24 h of RP using flow cytometry. This time point was chosen as previously shown to represent the peak of neutrophil accumulation after experimental ischemia in C57BL/6 wild type mice [9]. Immunostaining for CD45 and Ly6G allowed identifying side scatter $^{high}/CD45^{int}/Ly6G^{high}$ neutrophils as the major leukocyte subpopulation isolated from the ischemic hemispheres of both wild type and $ICAM\text{-}1^{null}$ C57BL/6 mice (Fig. 3a). Interestingly, irrespective of the presence or absence of ICAM-1, $Ly6G^{high}$ neutrophils isolated from the ischemic hemispheres displayed intermediate cell surface expression of CD45, which makes them distinct from circulating $Ly6G^{high}$ neutrophils expressing high cell surface levels of CD45 in the same animals (data not shown). Quantification of $CD45^{int}/Ly6G^{high}$ neutrophils isolated from the ischemic hemispheres of $ICAM\text{-}1^{null}$ C57BL/6 mice and wild type C57BL/6 mice at this time point was comparable (Fig. 3b). Thus, flow cytometry analysis of inflammatory cells isolated from the brain confirmed accumulation of comparable numbers of neutrophils in ischemic brain hemispheres of wild type and $ICAM\text{-}1^{null}$ C57BL/6 mice following 60 min ischemia and 24 h RP.

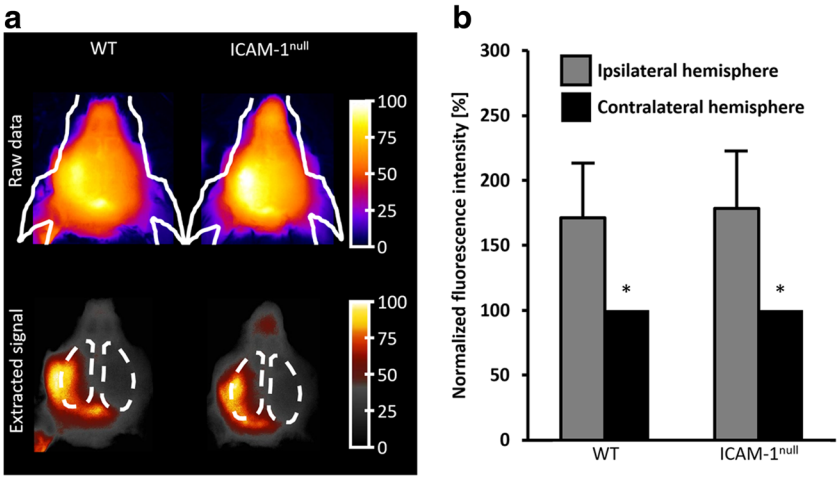

Fig. 2 In vivo tracking of NIRF labeled neutrophils after tMCAO. Representative in vivo NIRF images of epilated mouse heads are shown (**a**). Mice were imaged 19 h after adoptive transfer of LIPO-6S-IDCC-labeled neutrophils encompassing 60min of tMCAO and 18 h RP. The upper row shows the acquired images, the lower one the fluorescence signals after spectral unmixing, and the regions of interest drawn over the brain hemispheres. Normalized fluorescence intensities over the ischemic ipsilateral hemispheres and the contralateral hemisphere (**b**). Six wild type (WT) and 10 ICAM-1^{null} C57BL/6 mice were analyzed. Mean ± SD; Student's *t* test; $^{*}P < 0.05$ versus contralateral

Absence of ICAM-1 Does Not Alter the Spatial Distribution of Ly6G^{+}/CD45^{+} Neutrophils in the Ischemic Brain

Although absence of ICAM-1 did not affect the numbers of neutrophils accumulating in the ischemic brain, lack of ICAM-1 might still impact on neutrophil localization to different brain compartments and thus ultimately affect their contribution to stroke pathogenesis. To this end, we analyzed the localization of Ly6G^{+}/CD45^{+} neutrophils in brain sections of ICAM-1^{null} and wild type C57BL/6 mice at different time points after tMCAO. Our spatial and temporal analysis showed that individual Ly6G^{+}/CD45^{+} inflammatory cells accumulated in the brains not only of wild type but also of ICAM-1^{null} C57BL/6 mice as early as 6 h RP (not shown). Ly6G^{+} neutrophils were the first leukocytes detected to accumulate within the leptomeninges of the ischemic hemisphere of ICAM-1^{null} C57BL/6 mice, confirming our previous observations in wild type C57BL/6 mice [9]. The number of Ly6G^{+} neutrophils detectable within the ischemic hemisphere peaked at 24 h in wild type C57BL/6 mice and decreased thereafter (Fig. 4). In some but not all ICAM-1^{null} C67BL/6 mice, Ly6G^{+} neutrophils persisted longer and at slightly higher numbers in the leptomeningeal space (Fig. 4(f')). In general, the majority of Ly6G^{+} neutrophils was detected in the ipsilateral leptomeninges and was present from 6 to 48 h of RP in both wild type and ICAM-1^{null} C57BL/6 mice (Fig. 4(c, f, c', f')). Additional Ly6G^{+} neutrophils were found to accumulate intra- and perivascular with no overt differences observed between ICAM-1^{null} and wild type C57BL/6 mice (Fig. 4(a, d, a', d')). Furthermore, we always detected fewer Ly6G^{+} neutrophils in the basal ganglia compared to the adjacent cortex, irrespective of the genotype of the mouse (Fig. 4(b, e, b', e')). These observations suggest that absence of ICAM-1 in C57BL/6 mice did not affect neutrophil accumulation within leptomeningeal spaces or the neurovascular unit after ischemic stroke.

Absence of ICAM-1 Does Not Induce Compensatory Upregulation of Endothelial Cell Adhesion Molecules in Response to Ischemia and Reperfusion

It has been suggested that α4β1-integrin (VLA-4) can contribute to neutrophil accumulation in the brain after ischemic stroke [38]. To exclude that comparable accumulation of neutrophils in ischemic brains of ICAM-1^{null} and wild type C57BL/6 mice results from a compensatory upregulation of other adhesion molecules in brain endothelial cells, we performed immunostaining for ICAM-1, VCAM-1, and P-selectin in brain sections of ICAM-1^{null} and C57BL/6 mice wild type littermates. Immunostaining of ischemic brains of wild type mice revealed that ICAM-1 was upregulated on cerebral blood vessels at 6 h (not shown) and plateaued around 24 h of RP (Suppl. Fig. 1). ICAM-1 expression was observed in endothelial cells of the ischemic cortex, the striatum, and on meningeal vessels (Suppl. Fig. 1(a–c)) as well as on isolated blood vessels of the contralateral hemisphere (not shown). The absence of immunostaining for ICAM-1 in ICAM-1^{null} brains confirmed the complete lack of ICAM-1 in these mice (Suppl. Fig. 1(d–f)). Immunostaining for VCAM-1 followed a similar pattern as observed for ICAM-1 and was equally detected in cortical, striatal, and meningeal blood vessels of the lesioned hemisphere in ICAM-1^{null} and wild type mice (Suppl. Fig. 1(a'–f')). P-selectin immunostaining was

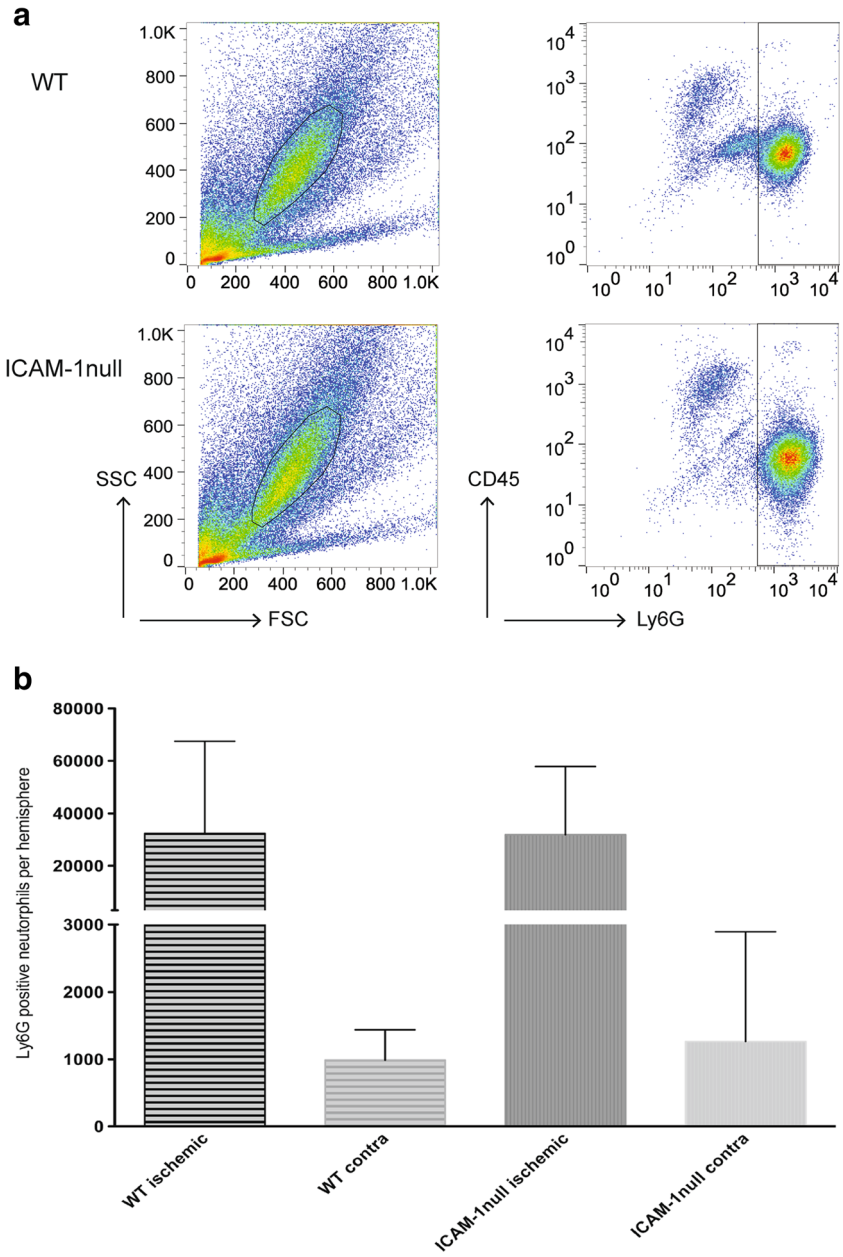

Fig. 3 Absence of ICAM-1 does not reduce the number of neutrophils accumulating in the ischemic brain. Flow cytometry analysis demonstrates the presence of $Ly6G^{high}$/$CD45^{intermediate}$ neutrophils in the ischemic brain after 60-min tMCAO and 24 h of reperfusion in both wild type (WT) and ICAM-1^{null} C57BL/6 mice (**a**). Quantitative flow cytometry analysis of $Ly6G^+$ neutrophils isolated from the ischemic brains revealed comparable numbers of accumulated $Ly6G^+$ neutrophils among $CD45^+$ cells in ICAM-1^{null} and WT C57BL/6 mice (**b**). The bars depict the number of $Ly6G^{high}$/$CD45^{intermediate}$ neutrophils isolated per hemisphere from four pooled brains per experiment and genotype investigated. Three independent experiments were performed and ipsilateral ischemic hemispheres were processed separately from the contralateral control each time. Data are presented as mean ± SD. No statistical significant differences (Student's *t* test, $P > 0.05$) were observed in the number of neutrophils isolated from the brains of WT and ICAM-1^{null} C57BL/6 mice post-ischemia

detected in meningeal but not in parenchymal blood vessel endothelial cells of the entire brain as observed before [35, 39]. At 6 h RP, P-selectin immunostaining was detected in leptomeningeal blood vessels and on platelets attached to vascular walls at a comparable manner in ICAM-1^{null} and wild type C57BL/6 mice. As the lesion matured, P-selectin immunostaining was also detected on cerebral vessels in various regions of the ipsilateral cortex and the striatum at 24 h RP in ICAM-1^{null} and wild type C57BL/6 mice (Suppl. Fig. 1(a", b", d", e")). In addition, we found upregulation of E-selectin on isolated vessels in the ipsilateral cortex and striatum following 12- to 24-h reperfusion but not in the contralateral hemisphere or in sham controls in both ICAM-1^{null} and wild type C57BL/6 mice (not shown). Taken together, we observed comparable kinetics, localization, and intensity in upregulation of VCAM-1 and E- and P-selectin on brain endothelial cells after ischemic stroke in ICAM-1^{null} C57BL/6 mice and wild type littermates.

Neutrophil Accumulation Does Not Correlate with Localized Upregulated Expression of Endothelial Cell Adhesion Molecules

We had previously observed that following cerebral ischemia $Ly6G^+$ neutrophils are trapped within the confines of the neurovascular unit and the leptomeninges [9]. To investigate if endothelial ICAM-1 contributes to neutrophil accumulation within the ischemic brain vessels, we performed double

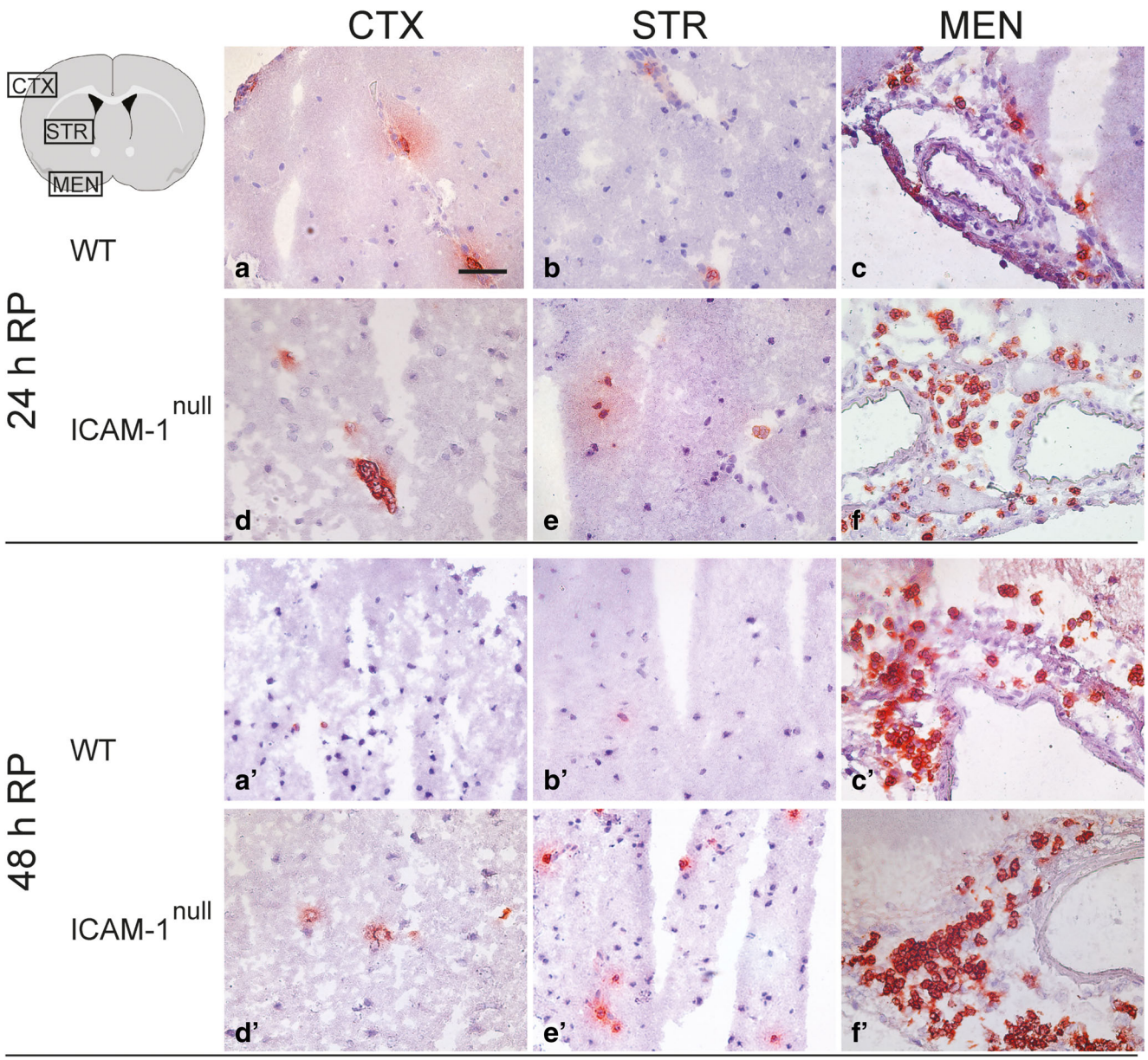

Fig. 4 Absence of ICAM-1 does not affect spatiotemporal accumulation of neutrophils in the ischemic brain. Representative images of the ischemic hemisphere of both wild type and ICAM-1^{null} C57BL/6 mice revealed accumulation of Ly6G^{+} neutrophils in parenchymal microvessels of the ipsilateral cortex (a, d) and the subarachnoidal space (c, f) at 24-h reperfusion after 60-min tMCAO. The number of vessel-associated Ly6G^{+} neutrophils declined sharply thereafter. Extensive edema is visible as vertical nicks on the tissue sections. Of note, Ly6G^{+} neutrophils were retained in the leptomeningeal compartment of wild type and ICAM-1^{null} C57BL/6 mice for an extended period of time (c', f'). The scale bar equals 50 μm

immunofluorescence staining for Ly6G and ICAM-1, VCAM-1, and P-selectin, respectively, allowing visualizing neutrophil localization in spatial correlation to localized enhanced expression of endothelial adhesion molecules (Suppl. Figs. 2–4). In general, Ly6G^{+} neutrophils were found in the leptomeningeal compartment and in parenchymal blood vessels irrespective of the presence of ICAM-1 and the time points of reperfusion (Suppl. Fig. 2), suggesting that ICAM-1 is not required for the spatial distribution of neutrophils in the ischemic brain. Additional immunostaining for VCAM-1 and P-selectin also failed to support a preferential localization of neutrophils to sites of upregulation of these known endothelial cell adhesion molecules as observed before [9]. We found neutrophils to localize to both VCAM-1 and P-selectin positive blood vessels (Suppl. Figs. 3(b') and 4(a', b')) as well as to blood vessels devoid of VCAM-1 or P-selectin immunoreactivity (Suppl. Figs. 3(a'), 4(b'–d')) in both wild type and ICAM-1^{null} C57BL/6 mice. Taken together, we found no preferential accumulation of neutrophils to sites of localized upregulated

expression of endothelial adhesion molecules as a consequence of cerebral ischemia irrespective of the absence or presence of ICAM-1.

Development of the Infarct Size Is Not Affected by the Absence of ICAM-1

Next, we asked whether the absence of ICAM-1 in C57BL/6 mice has any influence on the infarct size following transient ischemia/RP and measured the extent of the ischemic lesion in the ICAM-1^{null} C57BL/6 mice and wild type littermates on Cresyl Violet-stained brain sections. Irrespective of the investigated genotype, 60 min of ischemia caused comparable damage to the ischemic hemisphere. As highlighted in Fig. 5a, the lesion encompasses the basal ganglia, the somatosensory and motor cortex, various thalamic nuclei, and occasionally the hippocampus. Computer-assisted lesion volumetry did not reveal any significant difference in cerebral lesion volumes between ICAM-1^{null} and C57BL/6 wild type littermates (ICAM1^{null} 44.8 +/- 6.9 % versus wild type 45.1 +/- 11.1 % of the ipsilateral hemisphere)(Fig. 5b). These results demonstrate that absence of ICAM-1 is not neuroprotective following the 60-min ischemia/24-h reperfusion injury paradigm.

ICAM-1^{null} C57BL/6 Mice Are Prone to Increased BBB Leakage and Hemorrhagic Transformation After Ischemic Stroke

Impairment of the BBB contributes to stroke pathogenesis. Next, we therefore assessed whether the lack of ICAM-1 has any effects on the integrity of the BBB. To this end, we performed immunostaining for leakage of the endogenous plasma protein fibrinogen. We probed both the ischemic and contralateral hemisphere of wild type and ICAM-1^{null} C57BL/6 mice for extravasation of fibrinogen at different time points of RP. Figure 6 clearly indicates areas of altered BBB integrity in blood vessels of the lesioned cortex, the cerebral white matter, and the leptomeninges at 6 h RP (Fig. 6(a, e; a', e')). Of note, wild type and ICAM-1^{null} C57BL/6 mice that exhibited a higher neurological/functional impairment (Bederson score 3) displayed multiple foci with extravascular fibrinogen deposition (not shown). Assessing two wild type and three mutant stroke brains at 6-, 12-, 24-, and 48-h post-reperfusion, we

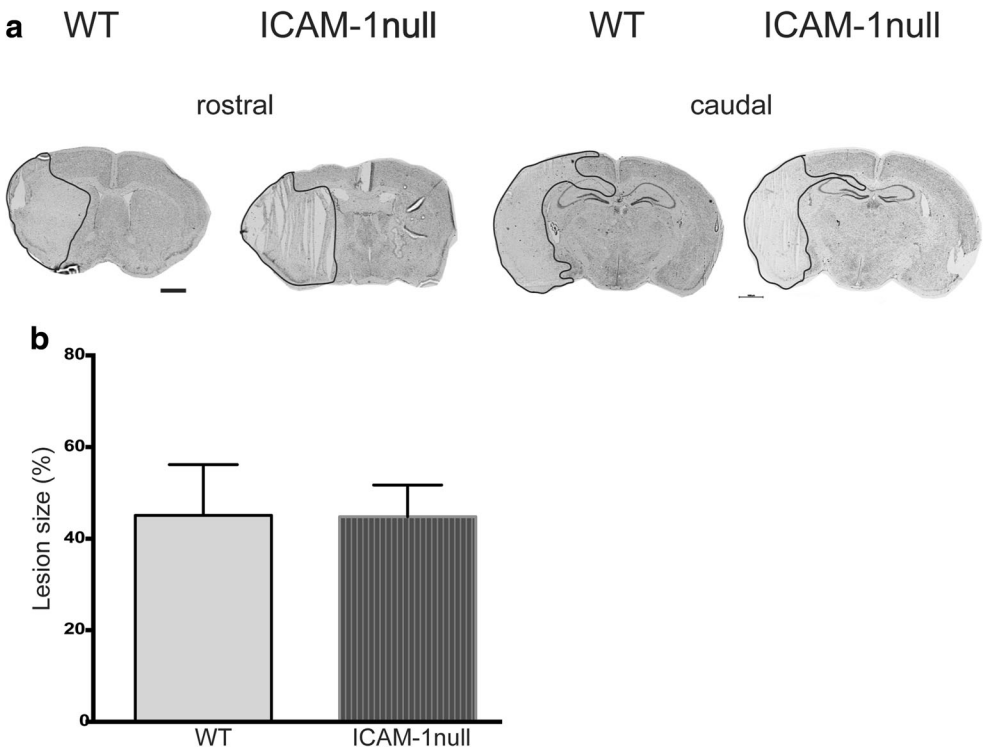

Fig. 5 Absence of ICAM-1 is not neuroprotective after 60-min tMCAO/24-h reperfusion. Cresyl Violet staining was applied to outline the infarcted area in C57BL/6 wild type (WT) and ICAM-1^{null} mice at 24-h reperfusion. Sections were taken at Bregma 0.38 mm (rostral) and − 1.70 mm (caudal) of one representative mouse per genotype (**a**). The scale bar equals 1 mm. Absence of ICAM-1 does not ameliorate the volume of spared brain tissue in the ipsilateral ischemic hemisphere compared to C57BL/6 WT littermates (**b**). A total of seven C57BL/6 WT and nine ICAM-1^{null} mice were analyzed, and the lesion volume was calculated after edema correction. Data are presented as mean ± SD. Student's *t* test was performed to compare different data sets and yielded no significant differences in the lesion size between WT and ICAM-1^{null} C57BL/6 mice ($P > 0.05$)

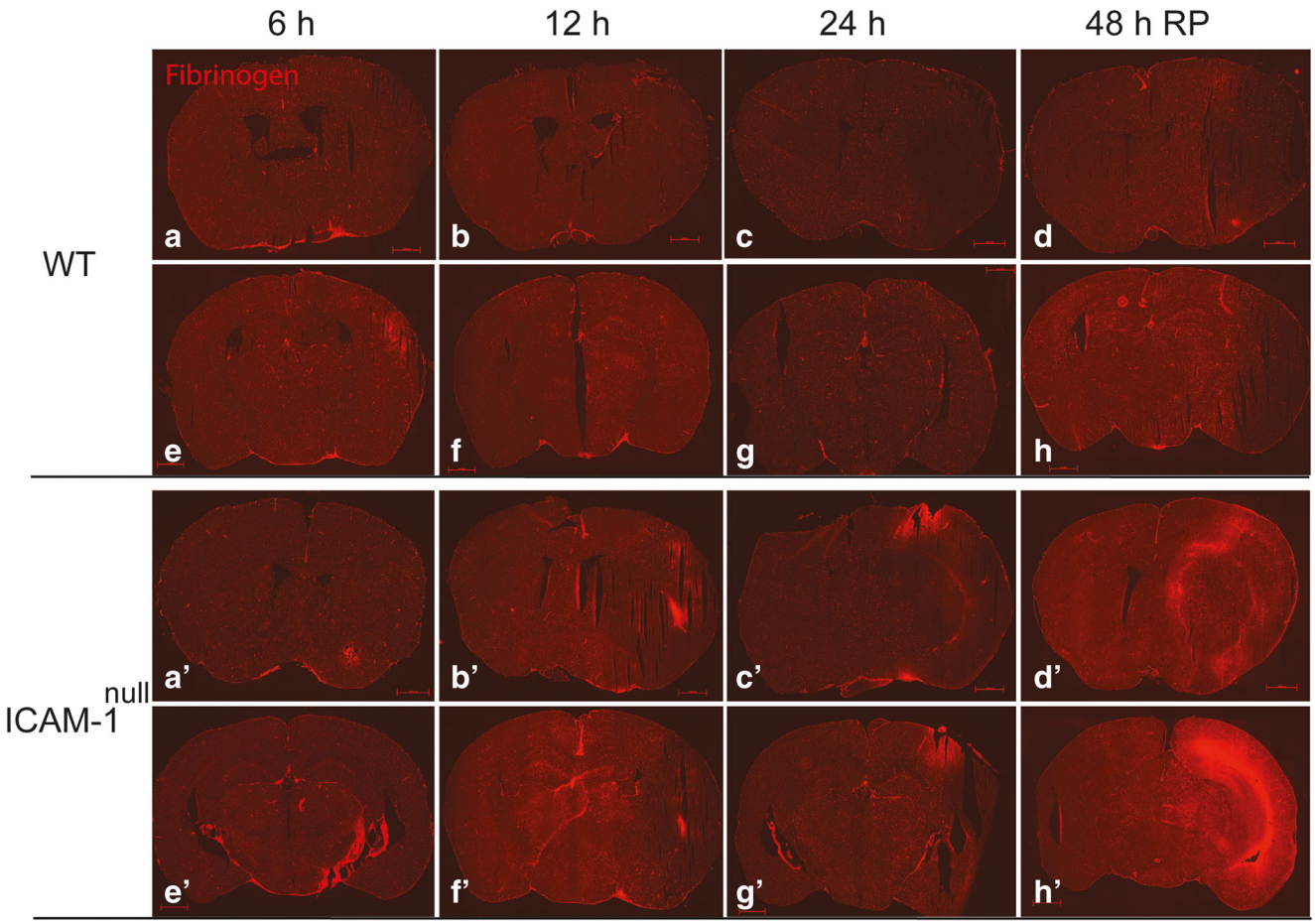

Fig. 6 ICAM-1^{null} C57BL/6 mice are prone to increased BBB damage. Immunofluorescence staining of brain sections showed multiple deposits of extravascular fibrinogen throughout the ischemic hemisphere of wild type (WT) and ICAM-1^{null} C57BL/6 mice indicating compromised BBB microvessels at 6-h reperfusion (a, e, a', e'). Fibrinogen leakage persisted longer and was more pronounced in ICAM-1^{null} C57BL/6 mice but not in brains of WT control mice at later time points of RP (b'–h', 6b–h). a–d and a'–d' display areas of BBB leakage in the rostral aspect of the ischemic brain whereas photomicrographs e–h and e'–h' show the caudal perimeter of the lesion. We assessed two wild type and three mutant stroke brains each at 6-, 12-, 24-, and 48-h reperfusion. All photomicrographs shown here originate from mice with a clinical disease score of "2." The scale bars equal 1 mm

observed that as the lesion matured, fewer but larger areas with BBB dysfunction especially in the ICAM-1^{null} C57BL/6 mice (Fig. 6(b', c,' e', f')).

Additionally, we observed a number of parenchymal blood vessels with altered morphology suggesting their disintegration in response to ischemia in wild type and ICAM-1^{null} C57BL/5 mice. To define the extent of damage in these vessels, we stained tissue sections for laminin, TER119, and Ly6G (Fig. 7) to outline the basement membranes of the respective vessels in relation to the localization of erythrocytes and neutrophils, respectively. Microscopic analysis suggested that neutrophils were released due to the rupture of blood vessels. The presence of parenchymal neutrophils was always accompanied by the presence of extraluminal erythrocytes (Fig. 7(b–c, a'–c')). Hemorrhagic transformation of cortical vessels was observed more frequently in ICAM-1^{null} C57BL/6 mice than in their wild type littermates (Fig. 7(a', a)). Specifically, seven out of 15 ICAM-1^{null} C57BL/6 mice exhibited parenchymal hemorrhages compared to only two out of 10 C57BL/6 wild type mice. Lesion volumes were not adversely affected in either cohort. Of note, immunohistological evaluation confirmed that a high number of neutrophils accumulating in the leptomeningeal space, irrespective of the genotype, always coincided with the presence of erythrocytes (Fig. 7(c', c)). Taken together, absence of ICAM-1 did not provide any protection from BBB breakdown or from hemorrhagic transformation of cortical vessels after ischemic stroke in C57BL/6 mice. Rather, ICAM-1^{null} C57BL/6 mice are prone to hemorrhagic transformation after experimental ischemic stroke.

Discussion

Understanding the contribution of neutrophils to the pathogenesis of stroke is of fundamental importance as treatment

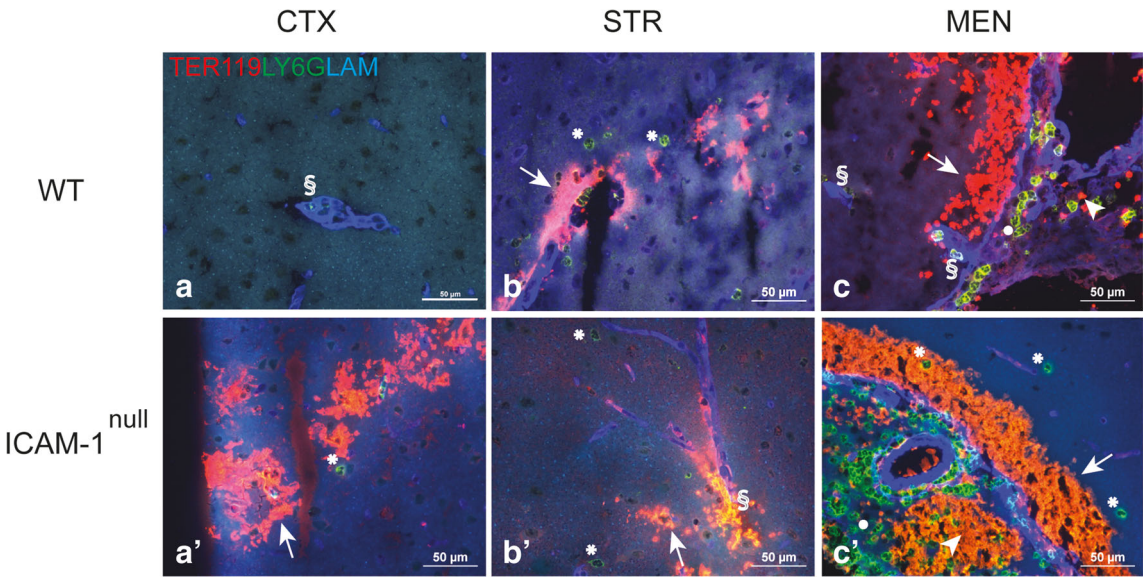

Fig. 7 ICAM-1^{null} C57BL/6 mice are prone to increased incidence of hemorrhagic transformation. Triple immunofluorescence staining shows damaged blood vessels by disrupted laminin staining (blue) and the presence of neutrophils (Ly6G, green) along extravascular erythrocytes (TER119, red). Hemorrhagic transformation of cortical blood vessels indicated by extraluminal erythrocytes occurred with higher frequency in the ischemic hemisphere of ICAM-1^{null} than wild type (WT) C57BL/6 mice (a, a', arrow) and is accompanied with release of neutrophils into the brain parenchyma (a', star). In detail, 47% of the 15 ICAM-1^{null} C57BL/6 mice (7/15 mice) exhibited parenchymal hemorrhages compared to only 20% C57BL/6 wild type mice (2/10 mice). Vessel disintegration was occasionally detected around the lenticulo-striate arteries of both genotypes (b, b'). There, neutrophils were detected intraluminal (§) and in the brain parenchyma (star) as well. Extraluminal erythrocytes (arrowheads) were observed in parallel to neutrophils (filled dots) in the subarachnoidal space of C57BL/6 WT and ICAM-1^{null} mice (c, c'). Copious amounts of erythrocytes (arrow) were accompanied by parenchymal neutrophils (star) in the superficial cortex of ICAM-1^{null} mice (c'). The scale bar equals 50 µm

options for cerebral ischemia are scarce. Experimental stroke models aimed at targeting neutrophil endothelial interaction and ameliorating disease progression raised hopes for clinical translation allowing improving the situation for stroke patients. Previously, Icam1^{tm1Jcgr} mutant C57BL/6 mice were shown to display improved cerebral blood flow and functional outcome as well as a reduction of the infarct volume when subjected to tMCAO [15]. Combined with the observation that neutrophil depletion ameliorated experimental stroke, these studies suggested an important role for ICAM-1-mediated neutrophil recruitment in the pathophysiology of an evolving stroke [15]. Unfortunately, a clinical study aimed to inhibit neutrophil adhesion to ischemic cerebral blood vessels by blocking endothelial ICAM-1 (R6.5) failed in humans [17]. A subsequent clinical trial targeting the β2-integrin subunit (CD18) of the ICAM-1 ligands αLβ2-integrin (LFA-1) and αMβ2-integrin (Mac-1) on neutrophils by a humanized antibody (Hu23F2G, LeukArrest) was suspended due to the absence of beneficial effects [18]. The ASTIN trial employed the glycoprotein UK-279,276 specifically targeting neutrophil αM-integrin (CD11b) in order to prevent neutrophil infiltration into the ischemic brain. Even though the treatment was well tolerated by the patients, it also failed to alleviate stroke severity and was therefore discontinued [40].

Recent findings from others and us have provided evidence that unlike previously thought following brain ischemia, the majority of neutrophils do not enter the brain parenchyma but are rather trapped in the leptomeninges and parenchymal blood vessels irrespective of RP [9, 14]. These findings suggest that adhesive contacts are formed between neutrophils and ischemic brain endothelium, however, fail to translate in neutrophil diapedesis across this barrier. Neutrophil arrest and crawling on the inflamed BBB is primarily mediated by interaction of neutrophil LFA-1 with ICAM-1 [29] ascribing ICAM-1 a pivotal role for neutrophil trapping post-ischemia. Absence of ICAM-1 should therefore prevent neutrophil endothelial interaction after ischemia.

In accordance to a previous study, MPIO conjugated anti-ICAM-1 antibodies decorated the targeted blood vessels in the ischemic mouse brain but did not interfere with the lesion development [41]. This is in line with our finding that both the number and the spatiotemporal pattern of neutrophil accumulation in the ischemic brain of ICAM-1^{null} C57BL/6 mice were indistinguishable from that observed in C57BL/6 wild type littermates. Our study therefore suggests that ICAM-1 does not play a predominant role in this process. An alternative explanation may be that endothelial and leukocyte ICAM-1 differentially influence neutrophil interaction with the BBB. Integrin activation is considered a two-step process starting with integrin extension followed by rearrangement in the ligand-binding site resulting in a high-affinity state of the molecule. Quantitative dynamic footprinting microscopy

combined with microfluidics recently described β2-integrins with a bent backbone but open headpiece on neutrophils, which can interact with ICAM-1 in *cis* orientation and prevent leukocyte adhesion [42]. It is tempting to speculate that absence of neutrophil ICAM-1 may abrogate its inhibitory effect on LFA-1 and cause post-stroke vascular accumulation of neutrophils to its endothelial ligands ICAM-1 and ICAM-2.

Alternatively, absence of ICAM-1 might be compensated by interaction of neutrophil very-late-antigen-4 (VLA-4, CD29/CD49d) with endothelial VCAM-1 as suggested by a recent study demonstrating that murine neutrophils express intermediate levels of VLA-4 in both the circulating population and the ischemic brain. However, cerebral ischemia itself is not sufficient to induce upregulation of neutrophil VLA-4 in either mouse or man [38]. While upregulation of VCAM-1 on endothelial cells in the parenchyma and leptomeninges of the ischemic hemisphere observed in the present study further supports a role for VLA-4/VCAM-1-mediated neutrophil accumulation in brain blood vessels after stroke, lack of a strict correlation of VCAM-1 immunostaining with vascular neutrophil accumulation suggests involvement of additional yet unidentified mediators.

ICAM-1 plays an important role in many immunological processes including leukocyte trafficking during health and disease or immunological synapse formation. The majority of studies have focused on analyzing the function of the type I transmembrane protein glycoprotein ICAM-1 with five extracellular Ig domains. In contrast, expression and function of the additional membrane-bound and soluble ICAM-1 isoforms that arise from alternative splicing and proteolytic cleavage during inflammatory responses is poorly understood. The ICAM-1^{null} mouse (Icam1^{tm1Alb}) used in the present study lacks expression of all ICAM-1 isoforms. In contrast, the two ICAM-1 mutants, Icam1^{tm1Jcgr} and Icam1^{tm1Bay}, still produce soluble alternatively spliced isoforms [24]. Soluble ICAM-1 is biologically active and affects leukocyte interaction with brain endothelium in vitro [22]. Most importantly, contrasting disease phenotypes of autoimmune neuroinflammation have been observed when studied in the different ICAM-1 mutant mice underscoring in vivo activity of soluble ICAM-1 splice variants [43]. In light of these findings, it is important to note that earlier studies in ICAM-1 mutant lines still expressing soluble ICAM-1 splice variants reported cerebral protection upon ischemic stroke [15, 16], while our present study in the complete absence of ICAM-1 isoforms failed to show such a protective effect. Taken together, this suggests a potential protective role of soluble ICAM-1 isoforms in ischemic stroke. To this end, our observation underscores that alternatively spliced ICAM-1 isoforms are functional in vivo and play key roles in the development of neuroinflammation also after ischemic stroke possibly by differential engagement of the ICAM-1 ligands LFA-1 and Mac-1 in leukocytes. The precise role of soluble ICAM-1 isoforms in neuroinflammation, however, awaits further studies.

Absence of ICAM-1 could ultimately affect stroke outcome by influencing BBB damage due to altered neutrophil accumulation or platelet aggregation. To determine BBB damage after ischemic stroke, we chose to study extravasation of the soluble serum glycoprotein fibrinogen that increases during inflammation. Its degradation products have been found to associate with increased BBB permeability [44, 45]. Following the development of the lesion over time revealed fibrinogen deposits in the ischemic somatosensory cortex and ventral aspects of the striatum. Barrier characteristics of brain microvessels in ICAM-1^{null} C57BL/6 mice were prone to a greater damage than those of C57BL/6 wild type littermates as indicated by widespread fibrinogen immunoreactivity in cortical structures and the hippocampus. Furthermore, we noted an increased incidence of hemorrhagic transformation upon stroke in ICAM-1^{null} compared to wild type C57BL/6 mice. While leptomeningeal hemorrhages occurred with a similar frequency (40%) in either genotype and were defined by the extraluminal presence of erythrocytes next to neutrophils, parenchymal hemorrhages were less frequent in C57BL/6 wild type mice but more numerous in the ischemic cortices of ICAM-1^{null} C57BL/6 mice (20 versus 47%) suggesting that absence of ICAM-1 promotes hemorrhagic transformation of the infarct. Indeed, adhesive interactions of platelets to microvascular walls have been shown in addition to PSGL-1/P-selectin and GPIIa/von Willebrand factor interactions to be mediated by the binding of platelet GPIIb/IIIa via fibrinogen to endothelial ICAM-1 (for review [46]). Experimental ablation of either fibrinogen or ICAM-1 reduces platelet accumulation (for review [46]), suggesting that upon ischemia, endothelial ICAM-1 might play a protective role by facilitating platelet adhesion and thus vascular fibrinogen deposition. Therapeutic targeting of ICAM-1 might thus bear the intrinsic risk of interfering with coagulation pathways ultimately leading to increased BBB impairment and hemorrhagic complications. How this may impact on the lesion size remains to be investigated, as we did not observe any significant difference in the lesion size between wild type and ICAM-1^{null} C57BL/6 mice.

Absence of parenchymal neutrophils around brain microvessels showing impaired barrier characteristics in our present study supports the notion that BBB dysfunction does not per se facilitate neutrophil transmigration into the ischemic hemisphere. Rather, presence of neutrophils in the brain parenchyma coincided with gross destruction of blood vessels in ICAM-1^{null} and wild type C57BL/6 mice suggesting their release from the circulation occurred in the absence of adhesion molecule-mediated controlled extravasation. In this context, it is interesting to note that disintegration of lenticulo-striate arteries, which are end-arteries and sensitive to fluctuation in blood pressure, was a

frequent source of neutrophils in the ventral aspect of the ischemic hemisphere of both ICAM-1^{null} and wild type C57BL/6 mice.

Finally, localization of neutrophils could be of functional importance to stroke outcome. Microscopic analysis of the temporal distribution of neutrophils during acute stroke defined the peak for neutrophil accumulation at 24 h RP. Neutrophils were predominantly accumulating in the leptomeninges, both at the luminal and abluminal sites of blood vessels. Fewer neutrophils were trapped within parenchymal blood vessels. Subsequently, neutrophils were no longer detected in parenchymal blood vessels but persisted in the leptomeninges in ICAM-1^{null} mice and C57BL/6 wild type littermates. Parenchymal neutrophils could rarely be observed. The accumulation of neutrophils in the leptomeningeal compartment and the Virchow-Robin space was previously observed in a rat model of permanent ischemia [14]. These authors suggested the leptomeningeal blood vessels as route of entry of neutrophils into the brain after prolonged occlusion in ischemic stroke. Considering the early time points when neuronal cell death is observed after ischemic stroke absence of neutrophils in transient ischemia and the late parenchymal arrival of neutrophils in permanent ischemia is however hard to reconcile with the assumption that neutrophil-mediated neuronal cell death requires their physical presence adjacent to the target cell.

Nevertheless, depletion of neutrophils has been shown to have beneficial effects on experimental stroke outcome [15, 38]. An intriguing explanation for these effects comes from experimental and clinical research on subarachnoid hemorrhages (SAH) pointing to a function of inflammatory leukocytes in the development of vasospasms (reviewed in [47]). In this context, the presence of neutrophils in the cerebrospinal fluid allowed predicting the development of delayed cerebral vasospasms in response to SAH [48]. Gr-1 antibody-mediated depletion of neutrophils and monocytes ameliorated development of cerebral vasospasms [49]. Ischemia has also been shown to induce constriction of capillary pericytes and arteriole smooth muscle cells thus critically regulating cerebral blood flow after stroke [50]. In accordance to the findings in SAH, it is tempting to speculate that vascular accumulation of neutrophils after ischemic stroke and local release of their inflammatory mediators might aggravate and extend microvascular constriction and thus BBB damage and ultimately neuronal cell death.

Taken together, our study fails to show a role for ICAM-1 in neutrophil accumulation in the brain after ischemic stroke. Rather, therapeutic targeting of ICAM-1 in stroke bears the risk of interfering with the coagulation cascade and hemorrhagic transformation. As the present study confirms neutrophil accumulation within the confines of the neurovascular unit and in the leptomeninges after ischemic stroke, the contribution of neutrophils to stroke pathogenesis might be localized to the vascular compartment and involve control of cerebral blood flow.

Acknowledgements We would like to thank the Microscopy Imaging Center (MIC) of the University of Bern, especially Dr. Roch-Philippe Charles (IBMM), for support in image analysis. We express our sincere thanks to Claudia Blatti, Therese Périnat, and Albert Witt for technical help in this study. We thank Dr. Urban Deutsch for help with the mouse breeding and genotyping logistics. Additional thanks go to Katrin Bissegger, Isabelle Wymann, and Svetlozar Tsonev for professional caretaking of the mice.

Author Contribution Statement G.E. and M.V. performed experiments including surgeries and data analysis, and G.E. wrote the manuscript. S.P. performed the experiments, analyzed the data, and prepared some figures. B.E. and J.K. outlined and supervised the project, evaluated data, and edited the manuscript.

Funding This study was funded by the EU FP7 European Stroke Network (grant nos. 201024 and 202213 to BE), the Swiss Heart Foundation (to BE and GE), and the Swiss National Science Foundation (grant PZ00P3_136822), and Hartmann-Müller Foundation (to JK).

Compliance with Ethical Standards

Ethical Approval All applicable international, national, and institutional guidelines for the care and use of animals were followed. In detail, in vivo experiments were approved by the Veterinary Office of the Canton of Bern (Switzerland) (licenses BE79/11, BE127/14). Animal research was performed in accordance to the Swiss legislation on the protection of animals and in compliance with the ARRIVE guidelines for reporting animal research (https://www.nc3rs.org.uk/arrive-guidelines).

Conflict of Interest The authors declare that they have no conflict of interest.

References

1. Neuwelt EA, Bauer B, Fahlke C, Fricker G, Iadecola C, Janigro D, et al. Engaging neuroscience to advance translational research in brain barrier biology. Nat Rev Neurosci. 2011;12(3):169–82. https://doi.org/10.1038/nrn2995.
2. Engelhardt B, Carare RO, Bechmann I, Flugel A, Laman JD, Weller RO. Vascular, glial, and lymphatic immune gateways of the central nervous system. Acta Neuropathol. 2016;132(3):317–38. https://doi.org/10.1007/s00401-016-1606-5.
3. Stanimirovic DB, Friedman A. Pathophysiology of the neurovascular unit: disease cause or consequence? JCBFM. 2012;32:1207–21.
4. Engelhardt B, Ransohoff RM. Capture, crawl, cross: the T cell code to breach the blood-brain barriers. Trends Immunol. 2012;33(12):579–89. https://doi.org/10.1016/j.it.2012.07.004.
5. Owens T, Bechmann I, Engelhardt B. Perivascular spaces and the two steps to neuroinflammation. J Neuropath Exp Neurol. 2008;67(12):1113–21. https://doi.org/10.1097/NEN.0b013e31818f9ca8.
6. Gelderblom M, Sobey CG, Kleinschnitz C, Magnus T. Danger signals in stroke. Ageing Res Rev. 2015;24(Pt A):77–82. https://doi.org/10.1016/j.arr.2015.07.004.
7. Barone FC, Feuerstein GZ. Inflammatory mediators and stroke: new opportunities for novel therapeutics. JCBFM. 1999;19:819–34.

8. Okada Y, Copeland BR, Mori E, Tung MM, Thomas WS, del Zoppo GJ. P-selectin and intercellular adhesion molecule-1 expression after focal brain ischemia and reperfusion. Stroke. 1994;25(1):202–11. https://doi.org/10.1161/01.STR.25.1.202.
9. Enzmann G, Mysiorek C, Gorina R, Cheng YJ, Ghavampour S, Hannocks MJ, et al. The neurovascular unit as a selective barrier to polymorphonuclear granulocyte (PMN) infiltration into the brain after ischemic injury. Acta Neuropathol. 2013;125(3):395–412. https://doi.org/10.1007/s00401-012-1076-3.
10. Jander S, Kraemer M, Schroeter M, Witte OW, Stoll G. Lymphocytic infiltration and expression of intercellular adhesion molecule-1 in photochemically induced ischemia of the rat cortex. JCBFM. 1995;15:42–51.
11. Garcia JH, Liu KF, Yoshida Y, Lian J, Chen S, del Zoppo GJ. Influx of leukocytes and platelets in an evolving brain infarct (Wistar rat). Am J Pathol. 1994;144(1):188–99.
12. Akopov SE, Simonian NA, Grigorian GS. Dynamics of polymorphonuclear leukocyte accumulation in acute cerebral infarction and their correlation with brain tissue damage. Stroke. 1996;27(10):1739–43. https://doi.org/10.1161/01.STR.27.10.1739.
13. Barone FC, Schmidt DB, Hillegass LM, Price WJ, White RF, Feuerstein GZ, et al. Reperfusion increases neutrophils and leukotriene B4 receptor binding in rat focal ischemia. Stroke. 1992;23(9):1337–47; discussion 47-8. https://doi.org/10.1161/01.STR.23.9.1337.
14. Perez-de-Puig I, Miro-Mur F, Ferrer-Ferrer M, Gelpi E, Pedragosa J, Justicia C, et al. Neutrophil recruitment to the brain in mouse and human ischemic stroke. Acta Neuropathol. 2015;129(2):239–57. https://doi.org/10.1007/s00401-014-1381-0.
15. Connolly ES Jr, Winfree CJ, Springer TA, Naka Y, Liao H, Yan SD, et al. Cerebral protection in homozygous null ICAM-1 mice after middle cerebral artery occlusion. Role of neutrophil adhesion in the pathogenesis of stroke. J Clin Invest. 1996;97(1):209–16. https://doi.org/10.1172/JCI118392.
16. Soriano SG, Lipton SA, Wang YF, Xiao M, Springer TA, Gutierrez-Ramos JC, et al. Intercellular adhesion molecule-1-deficient mice are less susceptible to cerebral ischemia-reperfusion injury. Ann Neurol. 1996;39(5):618–24. https://doi.org/10.1002/ana.410390511.
17. Investigators. Use of anti-ICAM-1 therapy in ischemic stroke: results of the Enlimomab Acute Stroke Trial. Neurol. 2001;57:1428–34.
18. Becker KJ. Anti-leukocyte antibodies: LeukArrest (Hu23F2G) and Enlimomab (R6.5) in acute stroke. Curr Med Res Opin. 2002;18(Suppl 2):s18–22. https://doi.org/10.1185/030079902125000688.
19. Xu H, Gonzalo JA, St Pierre Y, Williams IR, Kupper TS, Cotran RS, et al. Leukocytosis and resistance to septic shock in intercellular adhesion molecule 1-deficient mice. J Exp Med. 1994;180(1):95–109. https://doi.org/10.1084/jem.180.1.95.
20. Sligh JE Jr, Ballantyne CM, Rich SS, Hawkins HK, Smith CW, Bradley A, et al. Inflammatory and immune responses are impaired in mice deficient in intercellular adhesion molecule 1. Proc Nat Acad Sci USA. 1993;90(18):8529–33. https://doi.org/10.1073/pnas.90.18.8529.
21. van Den Engel NK, Heidenthal E, Vinke A, Kolb H, Martin S. Circulating forms of intercellular adhesion molecule (ICAM)-1 in mice lacking membranous ICAM-1. Blood. 2000;95:1350–5.
22. Rieckmann P, Michel U, Albrecht M, Bruck W, Wockel L, Felgenhauer K. Soluble forms of intercellular adhesion molecule-1 (ICAM-1) block lymphocyte attachment to cerebral endothelial cells. J Neuroimmunol. 1995;60(1-2):9–15. https://doi.org/10.1016/0165-5728(95)00047-6.
23. Hu X, Wohler JE, Dugger KJ, Barnum SR. Beta2-integrins in demyelinating disease: not adhering to the paradigm. J Leuk Biol. 2010;87(3):397–403. https://doi.org/10.1189/jlb.1009654.
24. Ramos TN, Bullard DC, Barnum SR. ICAM-1: isoforms and phenotypes. J Immunol. 2014;192(10):4469–74. https://doi.org/10.4049/jimmunol.1400135.
25. Dunne JL, Collins RG, Beaudet AL, Ballantyne CM, Ley K. Mac-1, but not LFA-1, uses intercellular adhesion molecule-1 to mediate slow leukocyte rolling in TNF-alpha-induced inflammation. J Immunol. 2003;171(11):6105–11. https://doi.org/10.4049/jimmunol.171.11.6105.
26. Bullard DC, Hu X, Schoeb TR, Collins RG, Beaudet AL, Barnum SR. Intercellular adhesion molecule-1 expression is required on multiple cell types for the development of experimental autoimmune encephalomyelitis. J Immunol. 2007;178(2):851–7. https://doi.org/10.4049/jimmunol.178.2.851.
27. Endres M, Fink K, Zhu J, Stagliano NE, Bondada V, Geddes JW, et al. Neuroprotective effects of gelsolin during murine stroke. J Clin Invest. 1999;103(3):347–54. https://doi.org/10.1172/JCI4953.
28. Bederson JB, Pitts LH, Tsuji M, Nishimura MC, Davis RL, Bartkowski H. Rat middle cerebral artery occlusion: evaluation of the model and development of a neurologic examination. Stroke. 1986;17(3):472–6. https://doi.org/10.1161/01.STR.17.3.472.
29. Gorina R, Lyck R, Vestweber D, Engelhardt B. Beta2 integrin-mediated crawling on endothelial ICAM-1 and ICAM-2 is a prerequisite for transcellular neutrophil diapedesis across the inflamed blood-brain barrier. J Immunol. 2014;192:324–37.
30. Vaas M, Enzmann G, Perinat T, Siler U, Reichenbach J, Licha K, et al. Non-invasive near-infrared fluorescence imaging of the neutrophil response in a mouse model of transient cerebral ischemia. JCBFM. 2017;37(8):2833–2847.
31. Reiss Y, Hoch G, Deutsch U, Engelhardt B. T cell interaction with ICAM-1-deficient endothelium in vitro: essential role for ICAM-1 and ICAM-2 in transendothelial migration of T cells. Eur J Immunol. 1998;28(10):3086–99. https://doi.org/10.1002/(SICI)1521-4141(199810)28:10<3086::AID-IMMU3086>3.0.CO;2-Z.
32. Engelhardt B, Laschinger M, Schulz M, Samulowitz U, Vestweber D, Hoch G. The development of experimental autoimmune encephalomyelitis in the mouse requires alpha4-integrin but not alpha4beta7-integrin. J Clin Invest. 1998;102(12):2096–105. https://doi.org/10.1172/JCI4271.
33. Borges E, Tietz W, Steegmaier M, Moll T, Hallmann R, Hamann A, et al. P-selectin glycoprotein ligand-1 (PSGL-1) on T helper 1 but not on T helper 2 cells binds to P-selectin and supports migration into inflamed skin. J Exp Med. 1997;185(3):573–8. https://doi.org/10.1084/jem.185.3.573.
34. Daley JM, Thomay AA, Connolly MD, Reichner JS, Albina JE. Use of Ly6G-specific monoclonal antibody to deplete neutrophils in mice. J Leuk Biol. 2008;83(1):64–70. https://doi.org/10.1189/jlb.0407247.
35. Doring A, Wild M, Vestweber D, Deutsch U, Engelhardt B. E- and P-selectin are not required for the development of experimental autoimmune encephalomyelitis in C57BL/6 and SJL mice. J Immunol. 2007;179(12):8470–9. https://doi.org/10.4049/jimmunol.179.12.8470.
36. Jalkanen S, Saari S, Kalimo H, Lammintausta K, Vainio E, Leino R, et al. Lymphocyte migration into the skin: the role of lymphocyte homing receptor (CD44) and endothelial cell antigen (HECA-452). J Invest Dermatol. 1990;94(6):786–92. https://doi.org/10.1111/1523-1747.ep12874646.
37. Engelhardt B, Conley FK, Kilshaw PJ, Butcher EC. Lymphocytes infiltrating the CNS during inflammation display a distinctive phenotype and bind to VCAM-1 but not to MAdCAM-1. Int Immunol. 1995;7(3):481–91. https://doi.org/10.1093/intimm/7.3.481.
38. Neumann J, Riek-Burchardt M, Herz J, Doeppner TR, Konig R, Hutten H, et al. Very-late-antigen-4 (VLA-4)-mediated brain invasion by neutrophils leads to interactions with microglia, increased ischemic injury and impaired behavior in experimental stroke. Acta

Neuropathol. 2015;129(2):259–77. https://doi.org/10.1007/s00401-014-1355-2.
39. Barkalow FJ, Goodman MJ, Gerritsen ME, Mayadas TN. Brain endothelium lack one of two pathways of P-selectin-mediated neutrophil adhesion. Blood. 1996;88(12):4585–93.
40. Krams M, Lees KR, Hacke W, Grieve AP, Orgogozo JM, Ford GA. Acute stroke therapy by inhibition of neutrophils (ASTIN): an adaptive dose-response study of UK-279,276 in acute ischemic stroke. Stroke. 2003;34(11):2543–8. https://doi.org/10.1161/01.STR.0000092527.33910.89.
41. Deddens LH, van Tilborg GAF, van der Marel K, Hunt H, van der Toorn A, Viergever MA, et al. In vivo molecular MRI of ICAM-1 expression on endothelium and leukocytes from subacute to chronic stages after experimental stroke. Transl Stroke Res. 2017;8(5):440–8. https://doi.org/10.1007/s12975-017-0536-4.
42. Fan Z, McArdle S, Marki A, Mikulski Z, Gutierrez E, Engelhardt B, et al. Neutrophil recruitment limited by high-affinity bent beta2 integrin binding ligand in cis. Nat Commun. 2016;7:12658. https://doi.org/10.1038/ncomms12658.
43. Hu X, Barnum SR, Wohler JE, Schoeb TR, Bullard DC. Differential ICAM-1 isoform expression regulates the development and progression of experimental autoimmune encephalomyelitis. Mol Immunol. 2010;47(9):1692–700. https://doi.org/10.1016/j.molimm.2010.03.005.
44. Carrano A, Hoozemans JJ, van der Vies SM, van Horssen J, de Vries HE, Rozemuller AJ. Neuroinflammation and blood-brain barrier changes in capillary amyloid angiopathy. Neurodegener Dis. 2012;10(1-4):329–31. https://doi.org/10.1159/000334916.
45. Tyagi N, Roberts AM, Dean WL, Tyagi SC, Lominadze D. Fibrinogen induces endothelial cell permeability. Mol Cell Biochem. 2008;307(1-2):13–22. https://doi.org/10.1007/s11010-007-9579-2.
46. Tailor A, Cooper D, Granger DN. Platelet-vessel wall interactions in the microcirculation. Microcirculation. 2005;12(3):275–85. https://doi.org/10.1080/10739680590925691.
47. Chaichana KL, Pradilla G, Huang J, Tamargo RJ. Role of inflammation (leukocyte-endothelial cell interactions) in vasospasm after subarachnoid hemorrhage. World Neurosurg. 2010;73(1):22–41. https://doi.org/10.1016/j.surneu.2009.05.027.
48. Provencio JJ, Fu X, Siu A, Rasmussen PA, Hazen SL, Ransohoff RM. CSF neutrophils are implicated in the development of vasospasm in subarachnoid hemorrhage. Neurocrit Care. 2010;12(2):244–51. https://doi.org/10.1007/s12028-009-9308-7.
49. Provencio JJ, Altay T, Smithason S, Moore SK, Ransohoff RM. Depletion of Ly6G/C(+) cells ameliorates delayed cerebral vasospasm in subarachnoid hemorrhage. J Neuroimmunol. 2011;232(1-2):94–100. https://doi.org/10.1016/j.jneuroim.2010.10.016.
50. Hall CN, Reynell C, Gesslein B, Hamilton NB, Mishra A, Sutherland BA, et al. Capillary pericytes regulate cerebral blood flow in health and disease. Nature. 2014;508(7494):55–60. https://doi.org/10.1038/nature13165.